Langmuir Article

pubs.acs.org/Langmuir

Structure of Solvent-Free Nanoparticle−Organic Hybrid Materials

Hsiu-Yu Yu and Donald L. Koch*

School of Chemical and Biomolecular Engineering, Cornell University, Ithaca, New York, 14853, United States

Received July 14, 2010. Revised Manuscript Received September 17, 2010

We derive the radial distribution function and the static structure factor for the particles in model nanoparticle−organic hybrid materials composed of nanoparticles and attached oligomeric chains in the absence of an intervening solvent. The assumption that the oligomers form an incompressible fluid of bead-chains attached to the particles that is at equilibrium for a given particle configuration allows us to apply a density functional theory for determining the equilibrium configuration of oligomers as well as the distribution function of the particles. A quasi-analytic solution is facilitated by a regular perturbation analysis valid when the oligomer radius of gyration R_g is much greater than the particle radius a. The results show that the constraint that each particle carries its own share of the fluid attached to itself yields a static structure factor that approaches zero as the wavenumber approaches zero. This result indicates that each particle excludes exactly one other particle from its neighborhood.

1. Introduction

Solventless nanoparticle−organic hybrid materials (NOHMs) are a new type of complex fluid composed of hard, inorganic nanocores with oligomeric chains covalently grafted to the surface of the core and with no other solvent molecules. The cores are self-suspended in a fluid phase of the attached oligomers, which in turn mediate the intercore forces. For typical polymer-stabilized micrometer-sized colloidal particles, the polymer mediated forces can be described using a pair interparticle potential. However, the absence of a solvent and the small size of the nanocores in NOHMs make their oligomer-mediated interactions non-pairwise-additive. To get insight into the thermodynamic, transport, and rheological properties of such a system, it is essential to first understand the structure and interparticle forces at equilibrium. The purpose of this paper is to formulate a theory that can estimate the equilibrium structure of homogeneous, liquid phase, solvent-free NOHMs without assuming a pairwise-additive interparticle potential.

NOHMs are a promising new class of materials whose unique physicochemical and transport properties have been demonstrated experimentally.[1−5] They provide a homogeneous nanoscale mixture of organic oligomers and inorganic cores. Unlike most nanoparticle systems which aggregate irreversibly due to strong van der Waals attraction, these surface functionalized nanostructures can relax to an equilibrium state and show liquid-like behavior in the absence of a solvent. One can calculate the van der Waals interaction between two equal spheres of radius a at a center-to-center separation r using $\Phi_{vdW} = -{}^1/_6 A\{[2a^2/(r^2 - 4a^2)] + [2a^2/r^2] + \ln[(r^2 - 4a^2)/r^2]\}$, with A being the Hamaker constant.[6] Since the intercore potentials arising from the entropy associated with the oligomer configurations are of $O(k_BT)$, with k_B being the Boltzmann constant and T being the temperature, the dimensionless number $W = \Phi_{vdW}/k_BT$ characterizes the magnitude of the van der Waals attraction relative to the oligomer free energy. For a typical solventless NOHMs system of silica cores with tethered polyethylene chains, the estimated nonretarded Hamarker constant would be about $0.1k_BT$ at 301 K given that the approximate dielectric constant and the refractive index are 3.91 and 1.45 for silica;[7] 2.26 and 1.482 for polyethylene.[8] For 10 nm diameter cores with a volume fraction of 0.3, the average interparticle spacing would be approximately the core radius and we obtain $W \approx 6 \times 10^{-4}$ at 301 K, indicating that the van der Waals interaction is much smaller than the oligomer-configurational entropy in such NOHMs systems. The goal of our study is to develop a theory of the many-core interactions arising from the entropy penalty incurred as the oligomers attempt to uniformly fill the space between the cores. We will see that the distribution of the cores arising from these interactions is more evenly spaced than a random hard sphere distribution. Such a uniform distribution occurs in ordered phases where each unit cell has a particle and its share of fluid space. However, here we have a disordered system that can act as a fluid but still has each particle surrounded by its share of the fluid, which is in fact attached to its surface. These features of NOHMs motivate the theoretical understanding of the intrinsic forces governing the equilibrium nanostructure of the system. We believe that NOHMs constitute an important new class of complex materials, and the present study is an initial attempt to develop a theory for their unique interactions and equilibrium structure.

Previous self-consistent field theories (SCFTs)[9−12] and scaling analyses[13−15] for particles with tethered molecules have emphasized

*To whom correspondence should be addressed. E-mail: dlk15@cornell.edu.

(1) Bourlinos, A. B.; Herrera, R.; Chalkias, N.; Jiang, D., D; Q., Z.; Archer, L. A.; Giannelis, E. P. *Adv. Mater.* **2005**, *17*, 234–237.
(2) Bourlinos, A. B.; Chowdhury, S. R.; Herrera, R.; Chalkias, N.; Jiang, D., D; Q., Z.; Archer, L. A.; Giannelis, E. P. *Adv. Funct. Mater.* **2005**, *15*, 1285–1290.
(3) Bourlinos, A. B.; Giannelis, E. P.; Q., Z.; Archer, L. A.; Floudas, G.; Fytas, G. *Eur. Phys. J. E* **2006**, *20*, 109–117.
(4) Rodriguez, R.; Herrera, R.; Q., Z.; Archer, L. A.; Giannelis, E. P. *Adv. Mater.* **2008**, *20*, 4353–4358.
(5) Agarwal, P.; Qi, H.; Archer, L. A. *Nano Lett.* **2010**, *10*, 111–115.
(6) Russel,W. B.; Saville, D. A.; Schowalter,W. R. *Colloidal Dispersions*; Cambridge University Press: New York, 1989.
(7) Yates, M. Z.; Shah, P. S.; Johnston, K. P.; Lim, K. T.; Webber, S. *J. Colloid Interface Sci.* **2000**, *227*, 176–184.
(8) Drummond, C. J.; Chan, D. Y. C. *Langmuir* **1997**, *13*, 3890–3895.
(9) Wijmans, C. M.; Zhulina, E. B. *Macromolecules* **1993**, *26*, 7214–7224.
(10) Lin, E. K.; Gast, A. P. *Macromolecules* **1996**, *29*, 390–197.
(11) Singh, C.; Pickett, G. T.; Zhulina, E. B.; Balazs, A. C. *J. Phys. Chem. B* **1997**, *101*, 10614–10624.
(12) Surve, M.; Pryamitsyn, V.; Ganesan, V. *Langmuir* **2006**, *22*, 969–981.
(13) Witten, T. A.; Pincus, P. A. *Macromolecules* **1986**, *19*, 2509–2513.
(14) Pincus, P. A. *Macromolecules* **1991**, *24*, 2912–1919.
(15) Badia, M.; Benhamou, M.; Derouiche, A.; Bretonnet, J. L. *Colloid Polym. Sci.* **2001**, *279*, 763–770.

attached polymers whose molecular weight was large under conditions where the particle interactions are pairwise additive. The tethered molecules are typically in a solution of added solvent or a melt of unattached polymers. In contrast, the attached molecules in NOHMs are oligomeric with typical lengths of 3−10 nm that are only a few times larger than the molecules' persistence length. In addition, the small O(5−10 nm) diameters of the cores and the absence of an added solvent imply that the oligomers from several neighboring cores will compete to fill the local interstitial space, leading to non-pairwise-additive intercore potentials. SCFTs and scaling analyses exploit a limit where the grafted polymers' contour length is large compared with the persistence length. In addition, monomer−monomer interactions are typically either neglected or incorporated only through a free energy penalty based on a virial expansion that is accurate when the attached molecules have a low volumetric concentration in a sea of added solvent. It would be difficult to accurately incorporate within these theories the constraint that the oligomers from several neighboring particles must form a nearly constant density fluid in the interstitial space. An attempt to accomplish this goal using SCFTs would lead to the need to solve a stiff set of integrodifferential equations in a complex interstitial geometry. The Daoud−Cotton (DC) model uses scaling concepts to provide a more analytical treatment of polymer chains grafted on convex surfaces and star polymers in good and theta solvents.[16] However, this theory again does not account for the space-filling nature of the chains. It has also been argued that the DC model does not correspond to a true minimum of the free energy of a curved brush.[17]

Several computational studies have considered nanoparticles with tethered oligomers in added phantom solvents. For instance, the polymer reference interaction site model (PRISM) has been applied to determine the effects of a single tether[18] or multiple tethers[19] on the structure of nanoparticles. In this approach, one solves an Ornstein−Zernike-like equation[20] for different site−site interactions with a chosen closure. The connected monomers within a chain are freely jointed. The colloid−colloid interaction is modeled as a Lennard-Jones-like pair potential, and only the hard sphere repulsion is assumed for colloid−monomer and monomer−monomer interactions. The hard-core monomer−monomer interactions can be considered to be applicable to a situation where the tethered oligomers are in a phantom solvent of monomers with the same chemical structure. Therefore non-pairwise-additive space-filling effects are not addressed. The pair correlation function and the structure factor obtained depend on the intercore attraction, positions and number of tethers, chain length, and particle volume fraction. Molecular dynamics simulations[21,22] for nanoscale colloids with a single tethered polymer have shown interesting phase behavior driven by the change in the chain configuration, polymer−colloid size ratio, and particle volume fraction. In these studies, a repulsive, truncated, and shifted Lennard-Jones pair potential is used for colloid−colloid interactions and bead−bead interactions. The neighboring beads within a polymer are either freely jointed or connected by harmonic springs. Again these studies correspond to colloids suspended in a phantom solvent. While these computational studies provide an initial indication of the interactions of nanoparticles with tethered branches, we will seek a more analytical treatment and one appropriate to a system without added solvent.

In the present study, we will treat the tethered oligomers as an incompressible fluid. That is to say that the concentration of monomers contributed by oligomers attached to all neighboring particles must be independent of position in the interstitial space. A test of the validity of this assumption can be made by comparing the entropic free energy associated with the translation of the cores to the work required to compress the oligomeric fluid. The isothermal compressibility χ (Pa^{-1}) of a fluid defined by $\chi = -(1/v)(\partial v/\partial p)_T$, with v being the molar volume of the fluid or mediate oligomers and p being the pressure, can be considered the inverse of the energy per unit volume required to compress the medium by an amount comparable with the system's current density. Thus, the reciprocal of the product of the compressibility and the number density of the particles (n_b^*) in the suspension characterizes the energy per particle required to compress the surrounding oligomers. A dimensionless number, $X = (\chi n_b^*)^{-1}/k_BT$, is the ratio of the energy to compress the oligomers to the thermal energy associated with the translation of the cores. For a suspension of 10 nm diameter cores with tethered polyethylene chains with $\chi \approx 5 \times 10^{-10}$ Pa^{-1} calculated from a Padé equation of state[23] and a core volume fraction of 0.3, $X \approx 10^6$ at 301 K. This indicates that the particle's thermal energy is insufficient to compress the intervening oligomeric fluid, which may then be considered incompressible.

The application of a hard incompressibility constraint using a Lagrange multiplier that we adopt in the present study is unusual in statistical mechanics. The typical procedure would be to specify the pairwise potential interactions among the monomers that make up the oligomers and deduce the configuration of the oligomers on this basis. In a liquid, however, the attractive interactions among the monomers along with their short-range repulsive forces lead to a monomer concentration that is very insensitive to pressure. It may be expected that the incompressibility condition would be approximated by conventional simulations and theories in the limit in which the attractive energy of the monomers becomes large compared with the thermal energy.

Polymers or oligomers tethered to particle surfaces in a good or theta solvent would typically be expected to yield a repulsive (steric) interaction between the particles. This interaction arises because the brush on one particle must be deformed due to the close proximity of the surface of the other particle. The incompressibility constraint on the total monomer concentration contributed by the molecules attached to all particles in the absence of an unattached solvent will be seen to yield a qualitatively new type of interparticle interaction. The absence of an unattached solvent and the incompressibility of the fluid phase imply that the space occupied by each particle and its attached oligomers must exclude exactly one neighboring particle with its attached oligomers. This constraint is equivalent to the statement that the static structure factor at zero wavenumber, which is related to the integral of the deviation of the conditional probability for finding a neighboring particle from the bulk number density, is zero, that is, $S(k^* = 0) = 1 + n_b^* \int_{V^*}[g(r_p^*) - 1]\mathrm{d}\mathbf{r}_p^* = 0$. Here, S is the static structure factor, k^* is the wavenumber, r_p^* is the interparticle distance, V^* is the suspension volume, $g(r_p^*)$ is the radial distribution function, and n_b^* is the bulk number density. It is well-known

(16) Marques, C. M.; Izzo, D.; Charitat, T.; Mendes, E. *Eur. Phys. J. B* **1998**, *3*, 353–358.
(17) Zhulina, E. B.; Birshtein, T. M.; Borisov, O. V. *Eur. Phys. J. E* **2006**, *20*, 243–256.
(18) Jayaraman, A.; Schweizer, K. S. *J. Chem. Phys.* **2008**, *128*, 164904.
(19) Jayaraman, A.; Schweizer, K. S. *Langmuir* **2008**, *24*, 11119–11130.
(20) Hansen, J.-P.; McDonald, I. R. *Theory of Simple Liquids*, 3rd ed.; Academic Press: London, 2006.
(21) Wilson, M. R.; Thomas, A. B.; Dennison, M.; Masters, A. J. *Soft Matter* **2009**, *5*, 363–368.
(22) Bozorgui, B.; Sen, M.; Miller, W. L.; Pàmies, J. C.; Cacciuto, A. *J. Chem. Phys.* **2010**, *132*, 014901.
(23) Sanchez, I. C.; Cho, J. *Polymer* **1995**, *36*, 2929–2939.

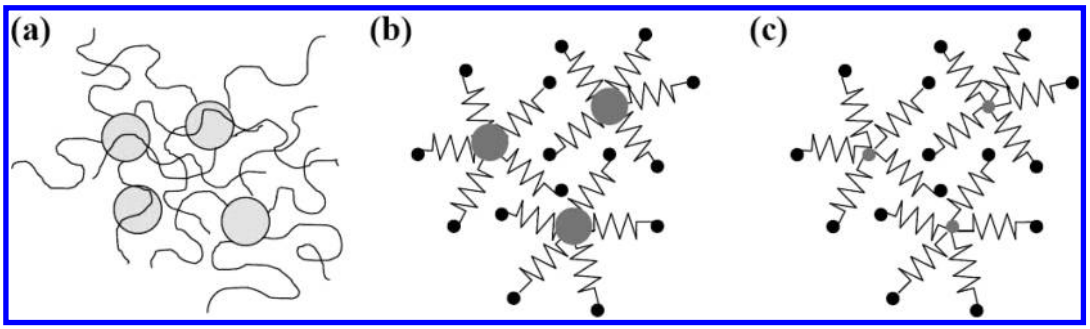

Figure 1. (a) Random particle array showing the oligomers can cross over several particles. (b) Schematic of the finite-core NOHMs model. The big central spheres are the hard cores, and the small beads represent the monomers. The monomers are connected to the core with springs, and each spring has one monomer. (c) Schematic of the point NOHMs model. The junction beads are the point cores with connected monomer beads. In our model, the number of oligomers per particle is an adjustable parameter M, and for clarity we only illustrate a few oligomers here.

that $S(k^* = 0) = 0$ in an *incompressible single-component fluid*.[20] However, $S(k^* = 0)$ is a finite value between zero and one in a disordered hard-sphere colloidal suspension and in typical disordered suspensions of particles with short-range repulsive forces such as those due to steric brush interactions. The facts that the incompressible fluid suspending the nanocores in NOHMs is attached to the cores and that each particle carries its own share of this fluid on its back imply that the system may be viewed as an *incompressible single-component fluid* with the component consisting of a particle plus its attached oligomers. As a result, the static structure factor for the *cores*, a quantity often observed in scattering experiments, will satisfy $S(k^* = 0) = 0$.

The static structure factor and the pair distribution function are interrelated. Thanks to Percus' observation,[24,25] the pair distribution function, that is, the radial distribution function, in a uniform classical fluid can be calculated from the one-body density profile when one fluid particle is fixed, that is, $n^*(\mathbf{r}_2^* - \mathbf{r}_1^*) = n_b^* g(\mathbf{r}_2^* - \mathbf{r}_1^*)$, where $n^*(\mathbf{r}_2^* - \mathbf{r}_1^*)$ is the density of fluid particles at $\mathbf{r}_2^*$ in a subensemble in which a particle is centered at $\mathbf{r}_1^*$. This concept has been widely used in the density functional theory, which successfully describes the structure of inhomogeneous simple fluids around a fixed entity.[26]

In this Article, we formulate a density functional theory for two simple coarse-grained models for pure NOHMs with bead-spring oligomers attached in the absence of other solvent molecules, one in which the cores are points and a second in which the finite hard-sphere radius of the core is taken into account. We first define the free energy of the oligomers for a given particle configuration. The equilibrium concentration field of the oligomers attached to a core is obtained by minimizing the oligomer free energy subject to the constraints that the field produced by the oligomers attached to an ith core is normalized and the oligomer fluid number density at a given $\mathbf{r}^*$ contributed from a sum of fields due to $i = 1,\ldots,N$ particles is independent of position throughout the fluid phase volume. These constraints of normalization and incompressibility along with the spring energy for the oligomers lead to an oligomer-configurational entropy penalty for large spaces between the core particles. Consequently, our results will be based on a different particle interaction mechanism than previous SCFTs work or the DC model, and conventional scaling laws for the polymer brush conformation in an unattached solvent will no longer be appropriate in such solvent-free systems.

(24) Percus, J. K. *Phys. Rev. Lett.* **1962**, *8*, 462–463.
(25) Lebowitz, J. L.; Percus, J. K. *J. Math. Phys.* **1963**, *4*, 248–254.
(26) *Fundamentals of Inhomogeneous Fluids*; Henderson, D., Ed.; Marcel Dekker: New York, 1992.

Analytical results for the concentration field are derived from a regular perturbation scheme under a "weak-field" approximation for the oligomer concentration. In particular, when the radius of gyration of the oligomers is large compared with the core radius ($R_g/a \gg 1$), many neighboring particles contribute oligomers to any fluid volume. As a result, the effect of each particle on the local oligomer concentration field is small. Use of the resultant, weak-field solution for the oligomer concentration field along with a density functional formulation allows a semianalytic determination of the radial distribution function and the static structure factor of cores. While our theory does not capture the details of intrachain excluded volume interactions, we will see that it does describe the changes in chain and core configurations caused by the requirement that all the chains from a test particle and neighboring particles must uniformly fill space.

2. Theory and Results

2.1. Point NOHMs. We first consider the case where the nanocores and oligomeric chains are modeled as point particles and bead-springs tethered to the central points, as shown in Figure 1c. The springs are linear, massless and have a rest length of zero. The spring energy is defined by $F_{spring} = {}^1/_2 \xi r^{*2}$ with ξ being the spring constant and r^* being the distance between the bead and the central point particle. The spring constant is chosen to be related to the radius of gyration R_g of an ideal, unattached linear chain as $\xi = k_B T/2R_g^2$. The probability distribution function of the bead, $G(\mathbf{r}^*) \sim \exp(-F_{spring}/k_B T)$, satisfies the normalization condition:

$$\int_{V^*} G(\mathbf{r}^*)\, d\mathbf{r}^* = 1 \tag{1}$$

The mean-square distance of the bead from the central point particle in the absence of chain−chain interactions is

$$\langle r*^2 \rangle = \int_{V^*} r*^2 G(\mathbf{r}^*)\, d\mathbf{r}^* = 6R_g^2 \tag{2}$$

Although the oligomers in NOHMs have only a moderate number of Kuhn steps, for simplicity we model them using an ideal chain wherein the radius of gyration is the sole parameter used for comparison with simulation and experiment. The basic form of the theory would be unaltered if a more sophisticated oligomer conformation model were adopted; this model would primarily alter the function G. All starred variables are dimensional radii, distances, volume, densities, and wavenumbers. Unstarred variables are nondimensionalized by R_g, and those with an overbar "−" are nondimensionalized by the core radius a.

The relaxation of the configuration of cores requires motion of all the oligomers attached to each core, while oligomer relaxation requires the motion of only one oligomer. Thus, the oligomers can relax quickly compared with the cores. Hence, we assume that for a given particle configuration the oligomers are at equilibrium. For a system of N particles, we write down the fluid phase free energy as (after replacing ξ by $k_BT/2R_g^2$)

$$\frac{F_f}{k_BT} = \sum_{i=1}^{N} \int_V C_i(\mathbf{r},\mathbf{r}_i)\left[\ln C_i(\mathbf{r},\mathbf{r}_i)\Lambda_b{}^3 - 1\right] + \frac{1}{4}(\mathbf{r}-\mathbf{r}_i)^2\, C_i(\mathbf{r},\mathbf{r}_i)\, d\mathbf{r} \quad (3)$$

where the first term represents the ideal gas Helmholtz free energy of the beads, the second term accounts for the spring energy, $C_i(\mathbf{r},\mathbf{r}_i)$ is the concentration field of the oligomers at $\mathbf{r}$ attached to particle i, $\mathbf{r}_i$ is the position of particle i, and Λ_b is the thermal de Broglie wavelength of the monomer beads. $C(\mathbf{r}) = \sum_{i=1}^{N} C_i(\mathbf{r},\mathbf{r}_i)$ is the total oligomer fluid number density at $\mathbf{r}$.

To determine the equilibrium concentration field of the oligomers, we must minimize the fluid phase free energy with respect to variations in C_i subject to the constraints that the probability of finding the oligomers attached to each particle is normalized,

$$\int_V C_i(\mathbf{r},\mathbf{r}_i)\, d\mathbf{r} = M \quad (4)$$

and the fluid number density is a constant in the suspension (incompressibility condition),

$$C(\mathbf{r}) = \sum_{i=1}^{N} C_i(\mathbf{r},\mathbf{r}_i) = n_bM \quad (5)$$

where M is the number of oligomers per core and $n_b\,[=n_b^*R_g^3]$ is the bulk number density of the cores. In mathematical optimization, one can make use of Lagrange undetermined multipliers to find a maximum or minimum of a function subject to constraints. A concise introduction to this technique can be found in ref 27. The Lagrange function for minimizing the free energy of NOHMs for a given core configuration subject to the normalization and incompressibility constraints is

$$L_f[C_i(\mathbf{r},\mathbf{r}_i)] = \frac{F_f}{k_BT} - \sum_{i=1}^{N} \lambda_i\left[\int_V C_i(\mathbf{r},\mathbf{r}_i)\, d\mathbf{r} - M\right] - \int_V \beta(\mathbf{r})\left[\sum_{i=1}^{N} C_i(\mathbf{r},\mathbf{r}_i) - n_bM\right] d\mathbf{r} \quad (6)$$

where the Lagrange multipliers λ_i enforcing the normalization make up a discrete set with one multiplier for each particle and the Lagrange multipliers $\beta(\mathbf{r})$ enforcing the incompressibility constraint are a continuous set or a function of position with the value of β at position $\mathbf{r}$ ensuring that the fluid number density at position $\mathbf{r}$ is equal to the average value, n_bM. For a given particle configuration, the minimization $\delta L_f/\delta C_i(\mathbf{r},\mathbf{r}_i)$ yields, after some manipulations and use of eq 4,

$$C_i(\mathbf{r},\mathbf{r}_i) = M\Lambda_iB(\mathbf{r})\, G(\mathbf{r}-\mathbf{r}_i) \quad (7)$$

where $B(\mathbf{r}) = e^{\beta(\mathbf{r})}$ accounts for the incompressibility, $G(\mathbf{r}-\mathbf{r}_i) = 1/(4\pi)^{3/2}\exp[-(\mathbf{r}-\mathbf{r}_i)^2/4]$, and Λ_i accounts for the normalization of the oligomers attached to particle i and other uninteresting factors not included in $B(\mathbf{r})$ or $G(\mathbf{r}-\mathbf{r}_i)$. We have made use of functional differentiations to minimize $L_f[C_i(\mathbf{r},\mathbf{r}_i)]$. Some physically oriented discussion of functional differentiations can be found in ref 20.

For the density functional theory, it will prove useful to define a conditional ensemble average of the oligomer concentration. We first specify the position of particle 1 as $\mathbf{r}_1$ and make it our *chosen* particle but consider all the other *nonchosen* particles labeled 2 as indistinguishable, then define the $(N-1)$-particle conditional ensemble average of a quantity A given that particle 1's center is fixed at $\mathbf{r}_1$ as $\langle A\rangle_1(\mathbf{r}|\mathbf{r}_1) = \int_V\cdots\int_V P^{(N-1)}(\mathbf{r}^{N-1}|\mathbf{r}_1)\, A(\mathbf{r})\, d\mathbf{r}_2\cdots d\mathbf{r}_N$. Applying the conditional ensemble average to the incompressibility constraint in eq 5 yields

$$\begin{aligned}\langle C\rangle_1(\mathbf{r}|\mathbf{r}_1) &= \int_V\cdots\int_V P^{(N-1)}(\mathbf{r}^{N-1}|\mathbf{r}_1)\left[C_1(\mathbf{r},\mathbf{r}_1) + (N-1)C_2(\mathbf{r},\mathbf{r}_2)\right]d\mathbf{r}_2\cdots d\mathbf{r}_N \\ &= \langle C_1\rangle_1(\mathbf{r}|\mathbf{r}_1) + (N-1)\int_V P^{(1)}(\mathbf{r}_2|\mathbf{r}_1)\langle C_2\rangle_2(\mathbf{r}|\mathbf{r}_1,\mathbf{r}_2)\, d\mathbf{r}_2 \\ &= n_bM \end{aligned} \quad (8)$$

where $\langle C_1\rangle_1(\mathbf{r}|\mathbf{r}_1)$ is the conditional average of the concentration field of oligomers attached to particle 1 given that particle 1 is fixed at $\mathbf{r}_1$, $\langle C_2\rangle_2(\mathbf{r}|\mathbf{r}_1,\mathbf{r}_2)$ is the conditional average of the concentration field of oligomers attached to particle 2 given that particles 1 and 2 are fixed at $\mathbf{r}_1$ and $\mathbf{r}_2$, $P^{(N-1)}(\mathbf{r}^{N-1}|\mathbf{r}_1)$ is the conditional probability density function of finding $N-1$ particles given that there is a particle fixed at $\mathbf{r}_1$, and $P^{(1)}(\mathbf{r}_1|\mathbf{r}_2)$ is the conditional probability density function of finding particle 2 at $\mathbf{r}_2$ given that there is a particle fixed at $\mathbf{r}_1$, which can be related to the radial distribution function by the relation $g(\mathbf{r}_2-\mathbf{r}_1)/V = P^{(1)}(\mathbf{r}_2|\mathbf{r}_1)$.

The conditional average of the incompressibility constraint with one particle fixed in eq 8 depends on the conditional average of the concentration of the oligomers of a second particle (particle 2) with two particle positions fixed. A conditional average of the incompressibility constraint with two particle positions held fixed would depend on an oligomer concentration field with three particle positions fixed and so forth. This leads to a closure problem which is common in ensemble average treatments of fields surrounding particles. One common method of achieving closure in theories for suspensions of particles in an unattached fluid solvent is to assume that the particles are dilute so that clusters of interacting particles are rare compared with isolated particles.[28,29] However, NOHMs are never dilute. In the absence of an unattached solvent, the oligomers of particle 1 must always be intertwined with the oligomers of its neighbors and one cannot achieve a small core particle concentration in which interactions are rare.

A second situation in which ensemble average field equations can be closed is one in which many particles contribute to the field in a certain region of space with no single particle having a disproportionate influence on the field. Under these circumstances, the contribution of each particle to the field is small. Furthermore, correlations of the field due to multiparticle interactions are weak compared with one-particle conditional averages. One precedent for this situation in the theory of particle suspensions is the fluid flow and chemical tracer dispersion in a dilute fixed bed of spheres.[29,30] In this case, the fluid velocity and tracer concentration fields produced by a particle are only truncated due to Brinkman

(27) McQuarrie, D. A. *Statistical Mechanics*; University Science Books: Sausalito, CA, 2000.

(28) Jeffrey, D. J. *Proc. R. Soc. London, Ser. A* **1973**, *335*, 355–367.
(29) Hinch, E. J. *J. Fluid Mech.* **1977**, *83*, 695–720.
(30) Koch, D. L.; Brady, J. F. *J. Fluid Mech.* **1985**, *154*, 399–427.

screening at a large distance from the particle, large enough to contain many neighboring particles.

The oligomer concentration field in NOHMs is influenced by many neighboring particles when the radius of gyration R_g of the oligomers is large compared with the interparticle spacing $n_b^{*-1/3}$, that is, $n_b^* {R_g}^3 = n_b \gg 1$. We will exploit this limit to close the equations governing the oligomer concentration and core pair probability distribution function in NOHMs. The B-field represents the influence of the incompressibility constraint on the concentration of the oligomers. When $n_b \gg 1$, the oligomer concentration contributed by particle i can readily be compensated by small $O(1/n_b)$ changes in the concentration of the oligomers attached to other particles and so the B-field deviates from 1 by only an $O(1/n_b)$ amount. Similarly, the surrounding particles have only a modest influence on the normalization constant required for particle i. Thus, we can write $B(\mathbf{r}) = 1 + B'(\mathbf{r})$ and $\Lambda_i = 1 + \Lambda_i'$ with $B'(\mathbf{r})$ and Λ_i' being of $O(1/n_b)$. It will be seen that these weak fields yield a weak perturbation to the free energy of the oligomers, resulting in a small change in the pair distribution function so that $g(\mathbf{r}_2 - \mathbf{r}_1) = 1 + h_f(\mathbf{r}_2 - \mathbf{r}_1)$ with $h_f(\mathbf{r}_2 - \mathbf{r}_1) = O(1/n_b)$. The weak-field approximation allows us to neglect nonlinear $O(1/{n_b}^2)$ terms such as $\Lambda_i' B'(\mathbf{r})$ compared with linear $O(1/n_b)$ terms such as $B'(\mathbf{r})$ or Λ_i'. Using this approximation, the conditional averages with one and two particles fixed of the solution for the oligomer concentration in eq 7 are

$$\langle C_1\rangle_1(\mathbf{r}|\mathbf{r}_1) \approx M[1 + \langle \Lambda_1'\rangle_1(\mathbf{r}_1|\mathbf{r}_1) + \langle B'\rangle_1(\mathbf{r}|\mathbf{r}_1)]G(\mathbf{r} - \mathbf{r}_1) \quad (9)$$

and

$$\langle C_2\rangle_2(\mathbf{r}|\mathbf{r}_1, \mathbf{r}_2) \approx M[1 + \langle \Lambda_2'\rangle_2(\mathbf{r}_2|\mathbf{r}_1, \mathbf{r}_2) + \langle B'\rangle_2(\mathbf{r}|\mathbf{r}_1, \mathbf{r}_2)]G(\mathbf{r} - \mathbf{r}_2) \quad (10)$$

When many particles ($O(n_b)$ particles) interact with a *chosen* particle, the correlation between the disturbances created by neighboring particles is weak. To quantify this concept, it is convenient to define a perturbation B'' to the B-field as $B'(\mathbf{r}) = B''(\mathbf{r}) + \langle B'\rangle_1(\mathbf{r}|\mathbf{r}_1) + \langle B'\rangle_1(\mathbf{r}|\mathbf{r}_2)$. Thus, B'' represents the perturbations to the B-field that are not captured by the conditional average B-field perturbations with particle 1 fixed and with particle 2 fixed separately. As a result, $\langle B''\rangle_2$ represents the B-field perturbations resulting from the correlations between particles 1 and 2. Since the perturbation caused by particle 1 is $O(1/n_b)$ and there are many ($O(n_b)$) particles interacting with particle 1, we expect that each of them will have a correlation $\langle B''\rangle_2 = O(1/{n_b}^2)$. Keeping terms up to $O(1/n_b)$, we can approximate the conditional average B-field with two particles fixed as a sum of one-particle fields

$$\langle B'\rangle_2(\mathbf{r}|\mathbf{r}_1, \mathbf{r}_2) \approx \langle B'\rangle_1(\mathbf{r}|\mathbf{r}_1) + \langle B'\rangle_1(\mathbf{r}|\mathbf{r}_2) \quad (11)$$

Similarly, the perturbation to the normalization constant of particle i can be written as $\Lambda_i' = \Lambda_i'' + \langle \Lambda_i'\rangle_1(\mathbf{r}_i|\mathbf{r}_i)$ where Λ_i'' is the deviation of particle i's normalization constant from the conditional average of this constant with particle i fixed. The conditional average of the normalization constant with two particles fixed is

$$\langle \Lambda_2'\rangle_2(\mathbf{r}_2|\mathbf{r}_1, \mathbf{r}_2) = \langle \Lambda_2'\rangle_1(\mathbf{r}_2|\mathbf{r}_2) + \langle \Lambda_2''\rangle_2(\mathbf{r}_2|\mathbf{r}_1, \mathbf{r}_2) \quad (12)$$

where up to $O(1/{n_b}^2)$ we can neglect the contributions of correlations with third particles to $\langle \Lambda_2''\rangle_2$.

After substituting eqs 9−12 into eq 8, we can equate terms of $O(n_b)$ and $O(1)$ to zero and neglect terms of higher orders. Applying the normalization condition for $\langle C_1\rangle_1$ and $\langle C_2\rangle_2$ and making use of Fourier transformations allow the $O(1)$ equation to only involve $\langle \hat{B}'\rangle_1$ in Fourier space. The characteristic length scale in this problem is R_g quantifying the range over which the disturbances to the field variables are important. Therefore, we scale the wavenumber with R_g such that $k = k^* R_g$, and upon Fourier transforming we obtain

$$\langle \hat{B}'\rangle_1(\mathbf{k}) = \frac{\hat{G}(\mathbf{k})[1 + n_b \hat{h}_f(\mathbf{k})]}{n_b[\hat{G}(\mathbf{k}^2) - 1]} \quad (13)$$

$$\langle \hat{\Lambda}_2''\rangle_2(\mathbf{k}) = -\langle \hat{B}'\rangle_1(\mathbf{k})\, \hat{G}(\mathbf{k}) \quad (14)$$

and

$$\langle \Lambda_i'\rangle_1(\mathbf{r}_i|\mathbf{r}_i) = -\frac{1}{(2\pi)^3}\int_{V_k} \langle \hat{B}'\rangle_1(\mathbf{k})\, \hat{G}(-\mathbf{k})\, \mathrm{d}\mathbf{k} \quad (15)$$

with V_k being all space in $\mathbf{k}$ and the subscript i is 1 or 2. Note that $\hat{G}$ is of $O(1)$ and $\hat{h}_f$ is of $O(1/n_b)$ as we have assumed, so $\langle \hat{B}'\rangle_1$ is of $O(1/n_b)$ as is shown explicitly in eq 13. The same is true for $\langle \hat{\Lambda}_2''\rangle_2$ and $\langle \Lambda_i'\rangle_1$. Since we have neglected terms of orders higher than $1/n_b$ in this analysis and proven the consistency of the order of magnitude, the perturbations to the field variables are correct to order $1/n_b$. The Fourier transform of $f(\mathbf{x})$ and the inverse transform of $\hat{f}(\mathbf{s})$ are defined by $\hat{f}(\mathbf{s}) = \int f(\mathbf{x})\, \mathrm{e}^{-i\mathbf{s}\cdot\mathbf{x}}\, \mathrm{d}\mathbf{x}$ and $f(\mathbf{x}) = [1/(2\pi)^3]\int \hat{f}(\mathbf{s})\, \mathrm{e}^{i\mathbf{s}\cdot\mathbf{x}}\, \mathrm{d}\mathbf{s}$.

We have solved for the conditional average concentration field of oligomers attached to a particle analytically. Our goal is to find the radial distribution function of the particles subject to the fluid phase free energy contributed from the oligomers. We can apply a density functional approach to achieve this. The essence of the density functional theory is to formulate an expression for the grand potential Ω, which is related to the Helmholtz free energy F_{Helm} of the entire system by $\Omega = F_{Helm} - \mu N$, with μ being the chemical potential of the particles. While the Helmholtz free energy is the thermodynamic potential of the canonical ensemble, the grand potential corresponds to the thermodynamic potential of the grand canonical ensemble.[27] If we follow Percus' observation,[24,25] when we fix a *chosen* particle labeled 1 at the origin, there will be a one-body density profile of other *nonchosen* particles labeled 2 around particle 1, $n(\mathbf{r}_p) = n_b g(\mathbf{r}_p)$, with $\mathbf{r}_p$ being $\mathbf{r}_2 - \mathbf{r}_1$. The grand potential is therefore a functional of this one-body density profile, $\Omega = F_{total} - \mu \int_V n(\mathbf{r}_p)\, \mathrm{d}\mathbf{r}_p$, and now F_{total} includes F_{Helm} and an additional "external" potential due to the fact that a particle has been fixed. This external potential can be determined if the fixed particle occupies a certain volume and interacts with other particles via a specific potential. In a NOHMs system with point cores interacting via a free energy due to the oligomers calculated by the equilibrium oligomer structure that we have determined, the external potential due to the fixed core is zero and the excess free energy contributed from the fixed particle's oligomers can be included within a part of the Helmholtz free energy denoted by F_{ex}. The grand potential is therefore written as

$$\Omega[n(\mathbf{r}_p)] = F_{id}[n(\mathbf{r}_p)] + F_{ex}[n(\mathbf{r}_p)] - \mu\int_V n(\mathbf{r}_p)\, \mathrm{d}\mathbf{r}_p \quad (16)$$

The ideal gas part of the free energy functional of the cores is

$$\frac{F_{id}[n(\mathbf{r}_p)]}{k_B T} = \int_V n(\mathbf{r}_p)\{\ln[n(\mathbf{r}_p){\Lambda_p}^3] - 1\}\, \mathrm{d}\mathbf{r}_p \quad (17)$$

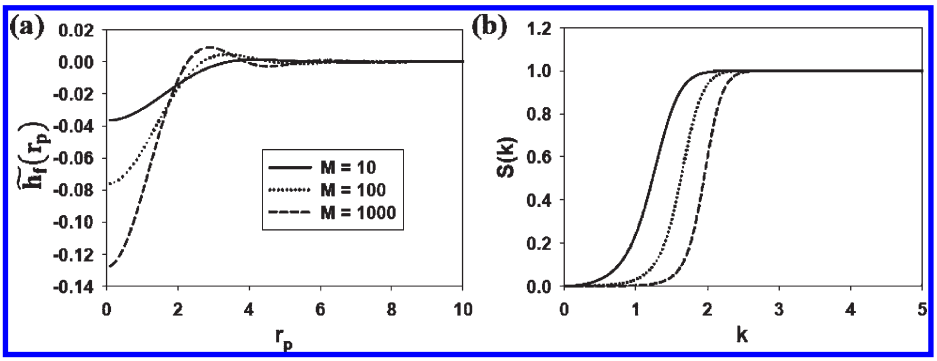

Figure 2. (a) Scaled perturbation to the pair probability $\tilde{h}_f (= n_b h_f)$ as a function of the interparticle distance r_p and (b) static structure factor S as a function of the wavenumber k for the point NOHMs model. M is the number of oligomers per core.

with Λ_p being the thermal de Broglie wavelength of the particles. For a given core configuration, the free energy of the oligomers is smeared out as a "mediated interparticle potential" (not the conventional pairwise one) between the cores. Mathematically, the excess free energy relative to the ideal gas is therefore the fluid phase free energy of the tethered oligomers conditionally averaged over the configuration of $N-1$ particles given that particle 1 is fixed at the origin,

$$\frac{F_{ex}[n(\mathbf{r}_p)]}{k_B T} = \left\langle \frac{F_f}{k_B T} \right\rangle_1 = \int_V \langle C_1 \ln C_1 \Lambda_b^3 \rangle_1(\mathbf{r}|\mathbf{0}) + \left[\frac{\mathbf{r}^2}{4} - 1\right] \langle C_1 \rangle_1(\mathbf{r}|\mathbf{0})\, d\mathbf{r} + \int_V n(\mathbf{r}_p) \int_V \langle C_2 \ln C_2 \Lambda_b^3 \rangle_2(\mathbf{r}|\mathbf{0}, \mathbf{r}_p) + \left[\frac{(\mathbf{r}-\mathbf{r}_p)^2}{4} - 1\right] \langle C_2 \rangle_2(\mathbf{r}|\mathbf{0}, \mathbf{r}_p)\, d\mathbf{r}\, d\mathbf{r}_p \tag{18}$$

where $\mathbf{r}_p$ is the position of particles labeled 2 relative to the origin and $\mathbf{r}$ is the position of the beads in the suspension relative to the origin.

At equilibrium, minimization of the grand potential $\delta\Omega[n(\mathbf{r}_p)]/\delta n(\mathbf{r}_p)$ and application of $\mu = \mu_{bulk} = \mu|_{\mathbf{r}_p \to \infty}$ yield

$$n(\mathbf{r}_p) = n_b\, g(\mathbf{r}_p) = n_b \exp\left\{ c^{(1)}(\mathbf{r}_p) - c_b^{(1)} \right\} \tag{19}$$

where $c^{(1)}(\mathbf{r}_p) = -\delta(F_{ex}[n(\mathbf{r}_p)]/k_B T)/\delta n(\mathbf{r}_p)$ is the so-called one-body direct correlation function evaluated at $\mathbf{r}_p$ and $c_b^{(1)} = -[\delta(F_{ex}[n(\mathbf{r}_p)]/k_B T)/\delta n(\mathbf{r}_p)]|_{\mathbf{r}_p \to \infty}$. The superscript "(1)" is to remind ourselves that the direct correlation function here is obtained from taking "one" functional derivative of F_{ex} and is for one particle, distinguished from the "two-body" direct correlation function used in literature of the integral equation theory. Under a weak-field approximation for the oligomers, we assume that the change in the excess free energy due to the change in particle configuration is of $O(1/n_b)$ and the exponent can be linearized such that we obtain

$$h_f(\mathbf{r}_p) \approx c^{(1)}(\mathbf{r}_p) - c_b^{(1)} \tag{20}$$

After substituting the field variables Λ_i and $B(\mathbf{r})$ into eq 18, we can neglect the correlations between the field variables caused by a second or third particle such that $\langle \Lambda_2''^2 \rangle_2 \approx \langle \Lambda_2'' \rangle_2^2$, $\langle B'^2 \rangle_1 \approx \langle B' \rangle_1^2$, $\langle \Lambda_2'' B' \rangle_2 \approx \langle \Lambda_2'' \rangle_2 \langle B' \rangle_2$, and so on based on the observation that multiparticle correlations are weak for $n_b \gg 1$ as discussed previously. Then functional differentiation $\delta(F_{ex}[n(\mathbf{r}_p)]/n_b k_B T)/\delta h_f(\mathbf{r}_p)$ with standard chain rules finally yields to $O(1/n_b)$,

$$h_f(\mathbf{r}_p) \approx 2M \int_V \langle \Lambda_2'' \rangle_2(\mathbf{r}_p'|\mathbf{0}, \mathbf{r}_p) \frac{\delta \langle \Lambda_2'' \rangle_2(\mathbf{r}_p'|\mathbf{0}, \mathbf{r}_p)}{\delta h_f(\mathbf{r}_p)}\, d\mathbf{r}_p' - 2M \int_V \langle B' \rangle_1(\mathbf{r}'|\mathbf{0}) \frac{\delta \langle B' \rangle_1(\mathbf{r}'|\mathbf{0})}{\delta h_f(\mathbf{r}_p)}\, d\mathbf{r}' \tag{21}$$

Since the changes in all the other particles' field variables due to the pair probability of a given pair of particles 1 and 2 are important only within a distance $\sim R_g$ from the fixed particle 1, we conclude that when particle 2 is deep in the bulk $\delta\langle \Lambda_2'' \rangle_2(\mathbf{r}_p'|\mathbf{0},\mathbf{r}_p)/\delta h_f(\mathbf{r}_p)$ and $\delta\langle B' \rangle_1(\mathbf{r}'|\mathbf{0})/\delta h_f(\mathbf{r}_p)$ are essentially zero, making the integrals in eq 21 convergent. Equation 21 contains convolution integrals which are simplified by Fourier transforming and using the convolution theorem. Making use of eqs 13 and 14, we thereby obtain

$$\hat{h}_f(\mathbf{k}) = -\frac{2M}{n_b} \left\{ \frac{\hat{G}(\mathbf{k})^2}{1 - \hat{G}(\mathbf{k})^2 + 2M\hat{G}(\mathbf{k})^2} \right\} \tag{22}$$

The prefactor $1/n_b$ shown explicitly again justifies the weak-field approximation. With this form of the perturbation to the pair probability in Fourier space, we can obtain the static structure factor of this one-component fluid defined by $S(\mathbf{k}) = 1 + n_b \int_V [g(\mathbf{r}_p) - 1] e^{-i\mathbf{k}\cdot\mathbf{r}_p}\, d\mathbf{r}_p = 1 + n_b \hat{h}_f(\mathbf{k})$[20] directly. When $\mathbf{k} \to \mathbf{0}$, we have $\hat{G}(\mathbf{0}) = 1$ and $S(\mathbf{0}) = 0$, which is consistent with the physical argument that each core in a solventless system must exclude one neighbor. The radial distribution function or the pair probability $g(\mathbf{r}_p)$ can be calculated by taking an inverse Fourier transform of $\hat{h}_f(\mathbf{k})$.

Figure 2 shows the scaled perturbation to the pair probability $\tilde{h}_f (= n_b h_f)$ and the static structure factor $S(k)$ for point NOHMs. The perturbation to the pair probability yields a decrease in the number of near neighbors and a slight increase in the number of neighbors at a distance of about three radii of gyration of the oligomers. As one might expect, these features become more pronounced as the number of oligomers per particle M is increased. Although we choose R_g to be the characteristic length scale quantifying the range of field interactions without treating the chain configurations explicitly, the "stronger" field observed in $\tilde{h}_f$ for more number of chains per core could also be rationalized by the more uniformly stretched oligomer brush resulting in a more structured pair probability. The decrease in the pair distribution function is relatively modest even when scaled with $1/n_b$. However, the deficit extends to sufficiently large distances allowing its volume integral to reach minus one so that each particle excludes one neighbor and $S(k = 0) = 0$. This may be

seen in Figure 2b where the static structure factor is plotted as a function of k for various M. In a suspension of point particles without tethered molecules, $S = 1$ throughout space. The onset of the deficit of neighboring particles, corresponding to a decrease in S with decreasing k, occurs at larger k values for larger M due to the stronger effects from the oligomers.

2.2. Finite-Core NOHMs. In this section, we model the structure of a suspension of NOHMs with finite cores having radius a and core volume fraction ϕ_b with bead-spring oligomers tethered to the centers of the cores as illustrated in Figure 1b. We consider linear springs whose rest length may be either zero or the core radius a. The spring energy of the springs with a rest length of a is $F_{spring} = {}^1/_2\xi(r^* - a)^2$. The normalization of the configurational probability of the oligomers and the definition of the mean-square distance of the chain from the center of the core are given by eq 1 and the first equality in eq 2. We will continue to use the radius of gyration of an ideal unattached spring with rest length zero and spring constant ξ, that is, $R_g = (k_BT/2\xi)^{1/2}$, to parametrize the stiffness of the oligomers even when discussing results for springs with rest length a.

We will consider the limit in which the radius of gyration is large compared with the core radius ${R_g}^3 \gg a^3$ and moderate core volume fractions $\phi_b \sim O(1)$. These conditions imply that $n_b^* {R_g}^3 = n_b \gg 1$ so that there are many neighboring particles within the distance R_g as there were in the point NOHMs model. The oligomers again cross many neighboring cores as illustrated in Figure 1a. In evaluating the pair distribution function, we can separate two length scales: the length scale a over which hard-core interactions influence the distribution of neighboring cores and the length scale R_g where most of a chosen particle's oligomers lie and over which those oligomers influence the probability of finding neighboring cores. Over the length scale R_g characteristic of the oligomer concentration field C_i, we can neglect the hard-core correlations and assume that the cores simply fill a fraction ϕ_b of the volume.

The condition $n_b \gg 1$ allows us to use a weak-field approximation in determining the oligomer concentration field, neglecting correlations smaller than $O(1/n_b)$ as was done in the point NOHMs model. The determination of the oligomer concentration field and the free energy due to the oligomers is then nearly identical to the treatment of the point NOHMs model in the previous section. We formulate the oligomer free energy and minimize it subject to constraints of normalization of the concentration of oligomers attached to a given core and incompressibility (or constant total oligomer concentration throughout space). This leads to a fluid phase free energy of the form of eq 3 except that the spring energy is now $\int_V {}^1/_4(|\mathbf{r} - \mathbf{r}_i| - a/R_g)^2 C_i(\mathbf{r},\mathbf{r}_i)\, d\mathbf{r}$ for the case where the rest length of the spring is a. The Lagrangian is still of the form eq 6, and the minimization of the Lagrangian $\delta L_f/\delta C_i(\mathbf{r},\mathbf{r}_i) = 0$ for a given particle configuration again yields the concentration field in the form of eq 7, where $G(\mathbf{r} - \mathbf{r}_i) = K_1 \exp[-{}^1/_4(|\mathbf{r} - \mathbf{r}_i| - a/R_g)^2]$ with K_1 being the normalization constant for G. Because most of the oligomers attached to a test particle are at an $O(R_g)$ distance from the particle center, we can allow G and the field variables Λ_i and B to be nonzero even within the core while making a small $O(a^3/{R_g}^3)$ error in the free energy. Applying the conditional ensemble average to the total concentration shown in eq 5 yields the incompressibility constraint eq 8.

To obtain an analytical solution to the oligomer concentration equations, we can exploit the limits ${R_g}^3 \gg a^3$ and $n_b \gg 1$, as we did for the point NOHMs model, to assume small perturbations from uniform fields, that is, $\Lambda_i = 1 + \Lambda_i'$ and $B(\mathbf{r}) = 1 + B'(\mathbf{r})$ with Λ_i' and $B'(\mathbf{r})$ being of $O(a^3/{R_g}^3)$. Neglecting the higher order correlations between the field variables as before, we can write $\langle C_1\rangle_1(\mathbf{r}|\mathbf{r}_1)$ and $\langle C_2\rangle_2(\mathbf{r}|\mathbf{r}_1,\mathbf{r}_2)$ as eqs 9 and 10. The incompressibility condition, eq 8, involves the pair distribution function, which is now influenced by both hard-core and oligomer-mediated core−core interactions. However, we will see that the weak oligomer fields imply that the pair probability can also be assumed to have a small $h_f = O(a^3/{R_g}^3)$ perturbation from a reference hard sphere distribution so that

$$g(\mathbf{r}_2 - \mathbf{r}_1) = 1 + h_{HS}(\mathbf{r}_2 - \mathbf{r}_1) + h_f(\mathbf{r}_2 - \mathbf{r}_1) \tag{23}$$

where h_{HS} is the total correlation function of the reference hard sphere suspension without the oligomers. Substituting eqs 9−12 and 23 into the incompressibility constraint (eq 8) results in $O({R_g}^3/a^3)$ and $O(1)$ equations that relate the field variables and the core pair probability. Specifically, the $O(1)$ equation is written as

$$\begin{aligned} G(\mathbf{r} - \mathbf{r}_1) + n_b \int_V [&\langle \Lambda_2'\rangle_1(\mathbf{r}_2|\mathbf{r}_2) + \langle \Lambda_2''\rangle_2(\mathbf{r}_2|\mathbf{r}_1,\mathbf{r}_2) + \langle B'\rangle_1(\mathbf{r}|\mathbf{r}_1) \\ &+ \langle B'\rangle_1(\mathbf{r}|\mathbf{r}_2) + h_{HS}(\mathbf{r}_2 - \mathbf{r}_1) + h_f(\mathbf{r}_2 - \mathbf{r}_1)] G(\mathbf{r} - \mathbf{r}_2)\, d\mathbf{r}_2 \\ &= 0 \end{aligned} \tag{24}$$

While h_f is $O(a^3/{R_g}^3)$ smaller than h_{HS}, h_f extends over a volume of order ${R_g}^3$ and h_{HS} extends only over a volume of order a^3, so that both terms make contributions of the same order to the Fourier transform of the field variables and to the static structure factor. Application of the normalization conditions for $\langle C_1\rangle_1$ and $\langle C_2\rangle_2$ and Fourier transformation of eq 24 eventually lead to

$$\langle \hat{B}'\rangle_1(\mathbf{k}) = \frac{\hat{G}(\mathbf{k})[1 + n_b\hat{h}_{HS}(\mathbf{k}) + n_b\hat{h}_f(\mathbf{k})]}{n_b[\hat{G}(\mathbf{k})^2 - 1]} \tag{25}$$

$\langle \hat{\Lambda}_2''\rangle_2(\mathbf{k})$ and $\langle \Lambda_i'\rangle_1(\mathbf{r}_i|\mathbf{r}_i)$ have the same relations (eqs 14 and 15) to $\langle \hat{B}'\rangle_1(\mathbf{k})$ as the point NOHMs model.

We again apply a density functional approach to solve for the radial distribution function. The grand potential Ω is similar to the point NOHMs model except that the excess free energy now has two terms: one is contributed from the hard spheres $F_{ex}^{HS}[n(\mathbf{r}_p)]$ and the other caused by the tethered oligomers filling the interparticle space $F_{ex}^{fluid}[n(\mathbf{r}_p)]$. Also, the grand potential now includes an external potential due to the hard-sphere excluded volume of the fixed *chosen* particle, $V_1(\mathbf{r}_p)$. Thus, the grand potential is

$$\begin{aligned} \Omega[n(\mathbf{r}_p)] = {} & F_{id}[n(\mathbf{r}_p)] + F_{ex}^{HS}[n(\mathbf{r}_p)] + F_{ex}^{fluid}[n(\mathbf{r}_p)] \\ & + \int_V n(\mathbf{r}_p)[V_1(\mathbf{r}_p) - \mu] d\mathbf{r}_p \end{aligned} \tag{26}$$

with F_{ex}^{fluid} being of the same form as eq 18 except that the spring energy of the oligomers attached to the fixed particle is now $\int_V [{}^1/_4(|\mathbf{r}| - a/R_g)^2 - 1]\langle C_1\rangle_1(\mathbf{r}|\mathbf{0})\, d\mathbf{r}$ and the spring energy of the oligomers attached to all the other particles is $\int_V n(\mathbf{r}_p) \int_V [{}^1/_4(|\mathbf{r} - \mathbf{r}_p| - a/R_g)^2 - 1]\langle C_2\rangle_2(\mathbf{r}|\mathbf{0},\mathbf{r}_p)\, d\mathbf{r}\, d\mathbf{r}_p$ if the rest length of the spring is a. The ideal gas free energy of the cores $F_{id}[n(\mathbf{r}_p)]$ also remains the same as eq 17. The minimization $\delta\Omega[n(\mathbf{r}_p)]/\delta n(\mathbf{r}_p) = 0$ and application of equal chemical potential of the neighboring particles, $\mu = \mu_{bulk} = \mu|_{\mathbf{r}_p \to \infty}$, yield

$$\begin{aligned} n(\mathbf{r}_p) &= n_b g(\mathbf{r}_p) \\ &= n_b \exp\left\{ c_{HS}^{(1)}(\mathbf{r}_p) - c_{HS,b}^{(1)} + V_1(\mathbf{r}_p) + c_f^{(1)}(\mathbf{r}_p) - c_{f,b}^{(1)} \right\} \end{aligned} \tag{27}$$

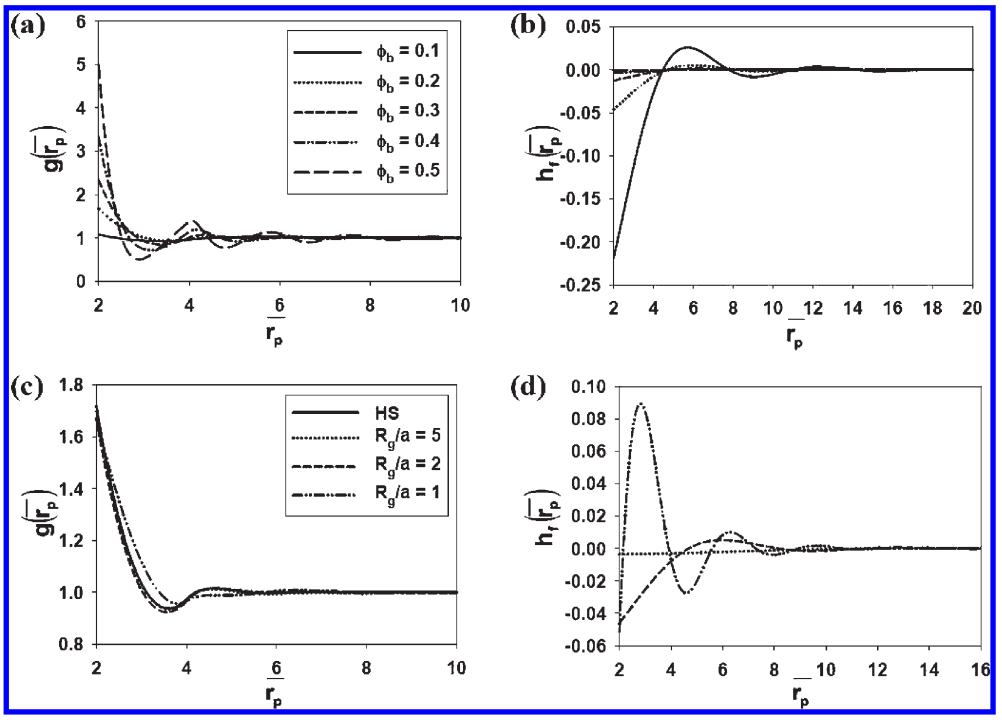

Figure 3. Results for the finite-core NOHMs model with zero-rest-length springs: (a) radial distribution function g as a function of the interparticle distance nondimensionalized by the core radius, $\bar{r}_p$, for different core volume fractions with $R_g/a = 2$ and (b) corresponding perturbation to the pair probability due to the oligomers, h_f, with the same parameters and curve descriptions as given in (a). (c) Comparison of g for different R_g/a and for a reference hard sphere suspension. The core volume fraction is 0.2. (d) Corresponding comparison of h_f.

where

$$c_{HS}^{(1)}(\mathbf{r}_p) = -\frac{\delta(F_{ex}^{HS}[n(\mathbf{r}_p)]/k_BT)}{\delta n(\mathbf{r}_p)}$$

$$c_{HS,b}^{(1)} = -\frac{\delta(F_{ex}^{HS}[n(\mathbf{r}_p)]/k_BT)}{\delta n(\mathbf{r}_p)}|_{\mathbf{r}_p\to\infty}$$

$$c_f^{(1)}(\mathbf{r}_p) = -\frac{\delta(F_{ex}^{fluid}[n(\mathbf{r}_p)]/k_BT)}{\delta n(\mathbf{r}_p)}$$

and

$$c_{f,b}^{(1)} = -\frac{\delta(F_{ex}^{fluid}[n(\mathbf{r}_p)]/k_BT)}{\delta n(\mathbf{r}_p)}|_{\mathbf{r}_p\to\infty}$$

Equation 27 implies that the pair probability can be expressed in the form $g(\mathbf{r}_p) = g_{HS}(\mathbf{r}_p)g_f(\mathbf{r}_p)$, where $g_{HS}(\mathbf{r}_p) = \exp[c_{HS}^{(1)}(\mathbf{r}_p) - c_{HS,b}^{(1)} + V_1(\mathbf{r}_p)] = 1 + h_{HS}(\mathbf{r}_p)$ is the radial distribution function of the reference hard sphere suspension with $h_{HS}(\mathbf{r}_p)$ being the corresponding total correlation function, and $g_f(\mathbf{r}_p) = \exp[c_f^{(1)}(\mathbf{r}_p) - c_{f,b}^{(1)}] = 1 + h_f(\mathbf{r}_p)$ can be viewed as an additional factor accounting for the change in the apparent core radial distribution function relative to the bare hard spheres due to the tethered oligomer fluid with $h_f(\mathbf{r}_p)$ being the total correlation function contributed from the oligomers. If we expand the product and write $g(\mathbf{r}_p) = 1 + h_{HS}(\mathbf{r}_p) + h_{HS}(\mathbf{r}_p)h_f(\mathbf{r}_p) + h_f(\mathbf{r}_p)$, we can see that $h_{HS}(\mathbf{r}_p)h_f(\mathbf{r}_p)$ is smaller than $h_{HS}(\mathbf{r}_p)$ in the inner region and negligible in the outer region where $h_f(\mathbf{r}_p)$ dominates. Therefore, we can neglect the cross term and obtain an expression for $g(\mathbf{r}_p)$ that is consistent with the form eq 23 assumed based on the regular perturbation expansion. Meanwhile, the separation of length scales implies that the change in $F_{ex}^{HS}[n(\mathbf{r}_p)]$ due to variations in $h_f(\mathbf{r}_p)$ is only an $O(a^3/R_g^3)$ perturbation to the change in $F_{ex}^{HS}[n(\mathbf{r}_p)]$ due to variations in $h_{HS}(\mathbf{r}_p)$ at separations of $O(a)$; while the change in $F_{ex}^{fluid}[n(r_p)]$ due to variations of $h_{HS}(\mathbf{r}_p)$ is essentially zero on the length scale of R_g because $h_{HS}(\mathbf{r}_p\to\infty)\to 0$. By keeping the dominant contributions from these variations of the free energy, we conclude that

$$c_f^{(1)}(\mathbf{r}_p) \approx -\frac{\delta(F_{ex}^{fluid}[n(\mathbf{r}_p)]/k_BT)}{n_b\delta h_f(\mathbf{r}_p)}$$

and

$$c_{HS}^{(1)}(\mathbf{r}_p) \approx -\frac{\delta(F_{ex}^{HS}[n(\mathbf{r}_p)]/k_BT)}{n_b\delta h_{HS}(\mathbf{r}_p)}$$

This is equivalent to neglecting the coupling between g_{HS} and g_f. Thus, we can use standard approaches in the literature to solve for g_{HS} without considering the effects due to the oligomer configuration. Conventional density functional approaches such as the weighted-density approximations (WDAs) have been used to solve for g_{HS}.[26] However, instead of using a density functional approach for g_{HS} in this Article, we directly evaluate it by solving the Ornstein−Zernike equation with the Percus−Yevick approximation.[20,27] Using the weak-field approximation, we can linearize the expression for g_f and obtain

$$h_f(\mathbf{r}_p) \approx c_f^{(1)}(\mathbf{r}_p) - c_{f,b}^{(1)} \tag{28}$$

Substitution of the field variables Λ_i and $B(\mathbf{r})$ into $F_{ex}^{fluid}[n(\mathbf{r}_p)]/k_BT$ shown in eq 18, truncation of the higher order correlations between the particles, and functional differentiation $\delta(F_{ex}^{fluid}[n(\mathbf{r}_p)]/k_BT)/n_b\delta h_f(\mathbf{r}_p)$ finally yield h_f in the same form as eq 21. After making use of the convolution theorem and the expressions for $\langle\hat{B}'\rangle_1(\mathbf{k})$ and $\langle\hat{\Lambda}_2''\rangle_2(\mathbf{k})$, in Fourier space we obtain

$$\hat{h}_f(\mathbf{k}) = -\frac{2M}{n_b}\left\{\frac{\hat{G}(\mathbf{k})^2[1+n_b\hat{h}_{HS}(\mathbf{k})]}{1-\hat{G}(\mathbf{k})^2+2M\hat{G}(\mathbf{k})^2}\right\} \tag{29}$$

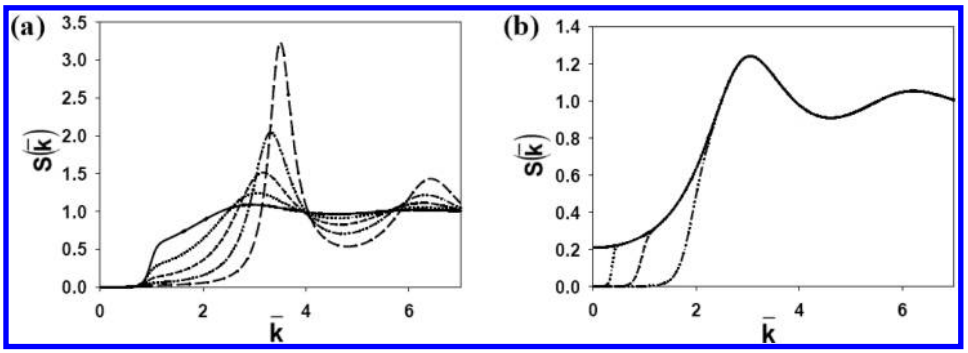

Figure 4. (a) Static structure factor S for the finite-core NOHMs with zero-rest-length oligomers as a function of the wavenumber nondimensionalized by the inverse core radius, $\bar{k}$, for different core volume fractions with $R_g/a = 2$. The lines are defined as in Figure 3a. (b) Comparison of S for finite-core NOHMs with different R_g/a ratios and the reference hard sphere suspension for a core volume fraction of 0.2. Lines are defined as in Figure 3c.

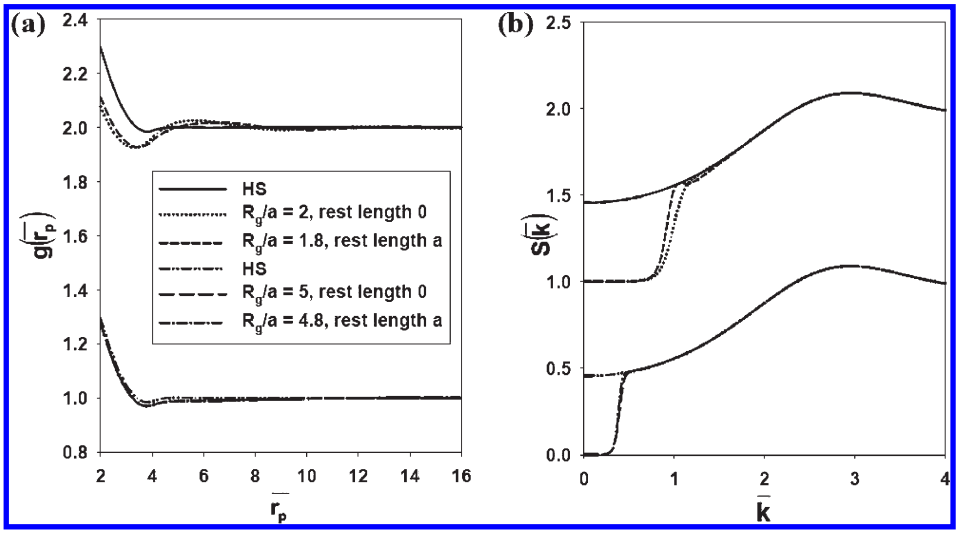

Figure 5. (a) Comparison of the radial distribution function g as a function of the interparticle distance $\bar{r}_p$ for models with different spring rest lengths for two R_g/a ratios and the reference hard sphere suspension when $\phi_b = 0.1$. The value of R_g/a for the model with nonzero rest length is adjusted so that the two models yield the same mean-square distance of the beads from the core center. (b) Corresponding comparison of the static structure factor S as a function of the wavenumber $\bar{k}$ with the same parameters and line definitions as in (a). Curves for different R_g are shifted vertically by 1 for clarity.

The static structure factor is now defined by $S(\mathbf{k}) = 1 + n_b\hat{h}_{HS}(\mathbf{k}) + n_b\hat{h}_f(\mathbf{k})$ and $S(\mathbf{0}) = 0$.

Results for the radial distribution function and static structure factor for finite-core NOHMs with the model of zero-rest-length springs are shown in Figures 3 and 4. To observe the hard-core contributions in a familiar way, the results are plotted as a function of the distance or wavenumber scaled by a. The core radial distribution functions in Figure 3a exhibit peaks similar to the hard sphere distribution. From the perturbation to the core pair probability h_f plotted in Figure 3b, we can see that the oligomer effects increase as the core volume fraction decreases. Experimentally,[4] for a fixed molecular weight of the tethered chains, the grafting density of the chains per particle changes when the weight percentage of the cores varies so that the oligomer fluid fills the space and yields a nearly constant fluid number density. Therefore, in the following calculations for the finite-core NOHMs model, we choose the number of oligomers per core as 600 when $\phi_b = 0.15$ to be consistent with the experiment and fix the fluid number density based on this chosen value; when we change the core volume fraction, the number of oligomers per core changes accordingly. When the core volume fraction is lower, we have more oligomer beads per particle so the field produced by the space-filling oligomers is more substantial and we obtain a stronger exclusion from the fixed particle. The effects of the oligomers on the static structure factor are more striking than their effects on the pair distribution function. In Figure 4a, we find two distinct length scales in the static structure factor. For large $\bar{k}$ values, the hard-core correlations dominate corresponding to the length scale of a; for small $\bar{k}$ values, a continuous deficit of the particles around the fixed particle due to the space-filling oligomers takes place on the length scale of R_g and enforces a zero $S(0)$. To probe the change in the structure due to the oligomer stiffness, we compare results with different oligomer radii of gyration and the purely hard spheres for a given ϕ_b in Figure 3c. The first peaks in $g(\bar{r}_p)$ for NOHMs are slightly damped, implying that the oligomers produce a *softened* potential. This *softening* becomes more important when R_g/a is smaller because the effects of stiffer oligomers are stronger. This can be confirmed by observing the perturbation to the core pair probability h_f presented in Figure 3d. As R_g/a decreases, h_f becomes more and more important and the positions of the peaks change with R_g. This can be rationalized by noting that, when R_g is shorter, the exclusion due to the fixed particle becomes more significant but on the other hand the entropic penalty of the oligomers makes a positive contribution to the probability of finding neighboring particles at close separation from the fixed particle. The corresponding $S(\bar{k})$ results for different radii of gyration in Figure 4b show two distinct length scales as in Figure 4a, characterizing different contributions from hard-core correlations and space-filling oligomers. Once more, we see $S(0) = 0$ for finite-core NOHMs. It is

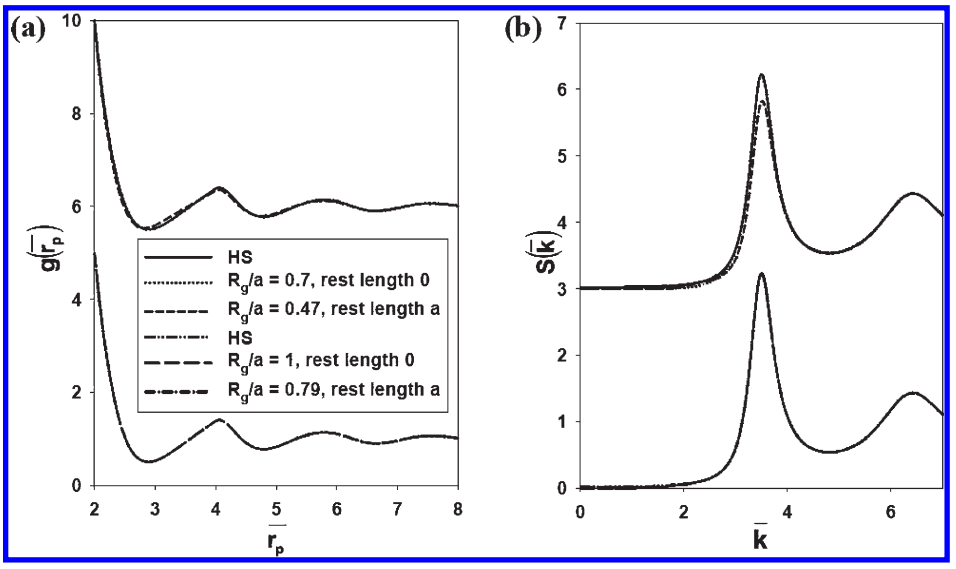

Figure 6. (a) Comparison of the radial distribution function g as a function of the interparticle distance $\bar{r}_p$ for models with different spring rest lengths for two R_g/a ratios and for the reference hard sphere suspension when $\phi_b = 0.5$. (b) Corresponding comparison of the static structure factor S as a function of the wavenumber $\bar{k}$ for the same parameters and line definitions as in (a). Curves for different R_g are shifted vertically by 5 for (a) and by 3 for (b).

noteworthy that $S(0)$ for the reference hard sphere suspension with the same ϕ_b does not go to zero. One can make it closer to zero by increasing the core volume fraction, but in general $S(0)$ is never zero for hard spheres immersed in a solvent. The continuous deficit of neighboring particles occurs at a higher $\bar{k}$ when R_g/a is smaller, showing a stronger penetration of the oligomer effects into the region where hard-core correlations occur if the oligomers are stiffer. Of course, the perturbation analysis will become less accurate as R_g/a decreases, but the model still provides physically reasonable results and we plan to test its accuracy by comparison with molecular dynamics simulations in a future study.

One might imagine that experimentally a slight deviation of $S(0)$ from zero could occur due to the intrinsic polydispersity in the core size and variations in the surface grafting density of the chains. We expect that a deficit in $S(k)$ would still occur in a polydisperse system at a similar length scale to that for a monodisperse system even if $S(0)$ deviates from zero, because this length scale is controlled by the oligomer chain length. In a future study, we will consider a NOHMs system with a bidispersity in the core size as well as the chain grafting density and compare with experimental measurements.

The constraint that the cores and oligomers must fill the volume of the suspension implies that the grafting density M in an experimental system must be changed while changing the particle volume fraction ϕ_b at fixed R_g/a. We took account of this effect in our calculations. The change in the volume filled by polymers with different R_g implies that M in an experimental system must also decrease with increasing R_g by an amount that depends on such details as the size of the monomer, the number of monomers per Kuhn step, and the number of Kuhn steps per oligomer. For simplicity, we have neglected this change in grafting density M with R_g in our calculations. From the results in Figure 2 for the point NOHMs system, one can see that the effect of M on the structure is weaker than the effect of R_g, so that the results in Figure 3c, d and the following Figures 5 and 6 would not be substantially altered by accounting for the changes in grafting density.

The qualitative behavior we have discussed remains the same for the model with the rest length of the springs being the core radius a. To make a reasonable comparison, the radii of gyration for the two models are chosen such that the calculated mean-square distances of the chain from the core center as defined by the first equality in eq 2 are the same. After calibrating the radius of gyration, we can see that the two models give very similar results. The difference in the quantitative results for the two models becomes more and more negligible when we have longer oligomers or higher core volume fractions. Specifically, we compare the two models for two different oligomer radii of gyration and the reference hard sphere system for $\phi_b = 0.1$ in Figure 5. When the mean-square distance is chosen such that $R_g/a = 5$ for the model with zero rest length springs, the two models exhibit basically the same g and S; when $R_g/a = 2$ for the zero-rest-length-spring model, the $S(k)$ plot exhibits an offset in the wavenumber at which the deficit of particles occurs and a slight phase shift and change in peak heights in g. If we push our calculations further to even smaller R_g/a values, as can be seen from Figure 6, when $\phi_b = 0.5$, the two models predict very similar structure of finite-core NOHMs. While differences in g and S are observable for the case of $R_g/a = 0.7$ for the zero-rest-length-spring model, the results for the two models basically coincide when $R_g/a = 1$. In this figure, the static structure factor for the reference hard spheres shows small but nonzero $S(0)$ because the core volume fraction is relatively high.

3. Conclusions

We have formulated a density functional approach to address the structure of a suspension of solvent-free nanoparticle−organic hybrid materials. Distinct from conventional theoretical treatments of equilibrium properties for complex materials in which a pairwise-additive potential is assumed, we propose a direct description of the fluid phase free energy functional as a mediated interparticle potential. With the widely used coarse-grained models such as point particles or finite hard cores with bead-spring oligomers attached, the radial distribution function and the static structure factor are solved in a quasi-analytical fashion exploiting a limit where the radius of gyration of the oligomers is large compared with the interparticle spacing. A simple estimate based on a typical oligomer's isothermal compressibility indicates that the mediate oligomer fluid is incompressible with a constant fluid number density. The effects due to these space-filling oligomers on the nanostructure become more substantial when the ratio between the oligomer radius of gyration and the core radius is smaller and/or the volume fraction of the

core is lower. Under all conditions of core volume fraction and oligomer radius of gyration, the static structure factor goes to zero for zero wavenumber. This reflects the fact that a particle carries its share of the fluid with it so that the particle and its oligomers fill a volume of space that excludes exactly one neighboring particle. While this situation is surprising from the perspective of colloidal science where particle cores typically exhibit nonzero $S(0)$, it is not surprising to the thermodynamicist who realizes that the nanoparticle−organic hybrid suspension constitutes an *incompressible single-component fluid*. Given a radial distribution function, one can also get insight into the non-pairwise-additive interparticle potential in such solventless systems by direct calculation of the potential of mean force defined by $V_{mf}(\bar{r}_p)/k_BT = -\ln g(\bar{r}_p)$.[20,27] V_{mf} therefore depends on the geometric parameters such as the core volume fraction, surface grafting density of the chains, as well as the size ratio between the chains and the cores.

Acknowledgment. This work was supported by Award No. KUS-C1-018-02, made by King Abdullah University of Science and Technology (KAUST).